Bulgarian Chemical Communications, Volume 50, Special Issue F (pp. 167–172) 2018

The effect of different acid stabilizers on the morphology and optical properties of ZrO_2 sol-gel films

O. Dimitrov[1*], I. Stambolova[2], K. Lazarova[3], T. Babeva[3], S. Vassilev[1], M. Shipochka[2]

[1] *Institute of Electrochemistry and Energy Systems, Bulgarian Academy of Sciences, G. Bonchev Str., bl. 10, 1113, Sofia, Bulgaria*
[2] *Institute of General and Inorganic Chemistry, Bulgarian Academy of Sciences, G. Bonchev Str., bl. 11, 1113, Sofia, Bulgaria*
[3] *Institute of Optical Materials and Technologies, Bulgarian Academy of Sciences, G. Bonchev Str., bl. 109, 1113, Sofia, Bulgaria*

Received October 16, 2018; Accepted December 03, 2018

Transparent and homogeneous ZrO_2 films were obtained by sol-gel technique using different acids as stabilizing agents. Tetragonal ZrO_2 phase with small nanosized crystallites is characteristic for the studied films. The surface morphology of the samples is smooth and continuous without visible cracks. An average transmittance of about 80% was observed for the samples in the visible range. The refractive indexes of the films prepared using CH_3COOH and HNO_3 are 1.672 and 1.602, respectively. The chemical composition of the films as revealed by XPS analysis show the presence of oxygen defects. Photoluminescence (PL) properties were also studied in the range of 300–550 nm. The PL spectra of the samples obtained from solutions with CH_3COOH and HNO_3 exhibit broad emission band with maximum at 401 and 415 nm, respectively. The later PL peak has stronger intensity, due to the larger size of crystallites of the HNO_3 films, as opposed to the CH_3COOH samples.

Keywords: zirconia, thin films, chelating agents, photoluminescence.

INTRODUCTION

Zirconium thin films exhibit unique physicochemical properties: thermal and chemical stability, high hardness, corrosion resistance, high refractive index, biocompatibility etc. These properties make them attractive material for application in optoelectronic devices [1], thermal and corrosion protection coatings [2], wear resistance coatings [3], sensors [4] and bio implants [5]. Various physical and chemical methods for preparation of zirconia films are applied: plasma spraying [6], RF sputtering [7], pulsed laser deposition [8], chemical vapor deposition (CVD) [9], electrochemical deposition [10], spray pyrolysis method [11] and sol-gel method [12]. The sol-gel method is a wet-chemical low temperature method, based on hydrolysis and condensation reactions [13]. At present the classical sol-gel process is one of the most appropriate technology for preparation of homogeneous, uniform and high quality ZrO_2 films [14, 15] and powders [16, 17]. The proper selection of the type of chelating agent and acid catalysts is very important in order to control the hydrolysis and condensation reaction rates of the metal alkoxide and the preparation of a stable sol, which affects the films properties and uniformity. Various chelating agents (diethanolamine [1], acetic acid [14], acetylacetone [18] and strong acids such as hydrochloric acid or nitric acid [19, 20]) have been used. In the available literature, very few articles are devoted to the influence of chelating agents and acids on the photoluminescence properties of ZrO_2 sol-gel films. Lakshmi et al. have revealed that ZrO_2 films, deposited from zirconium butoxide and acetylacetone possess intrinsic defects, which are responsible for the luminescence properties [21]. Vinogradov et al. have revealed that both nucleation and phase composition of sol-gel TiO_2 films are influenced by the addition of acids with different degrees of dissociation [22]. The aim of this paper is to investigate for the first time the effect of addition of weak or strong acid as stabilizing agents on the photoluminescence and morphology of ZrO_2 nanosized films.

* To whom all correspondence should be sent:
Email: ognian.dimitrov@iees.bas.bg

EXPERIMENTAL

Zirconium n-butoxide n-butanol complex ($(C_4H_9O)_4Zr.C_4H_9OH$), Alfa Aesar) was used as a zirconium precursor, which was diluted in isopropanol up to 0.25M under vigorous stirring for 30 min. In order to investigate the effect of the chelating agents and/or catalyst two types of solutions were made: one using acetic acid (CH_3COOH) as stabilizing agent and one using nitric acid (HNO_3). The molar ratio Zr:CH_3COOH was 1:1, while Zr:HNO_3 was set to 4:1. Two types of substrates were used: microscope glass (Waldemar Knittel, 3×1 inch) and Si wafers. The films were deposited by sol-gel method using dip coating technique with an experimental procedure shown on Fig. 1. The substrates were dipped into the corresponding precursor solution and after 20 sec at fully submerged position (to ensure better wettability) they were pulled out with constant withdrawal speed of 3 cm/min. The thin films were dried at 150 °C for 10 min in air. These steps were repeated 5 times to obtain the corresponding thickness. After the fifth dipping/drying cycle the samples were annealed at 500 °C for 1h in air. Utilizing this experimental procedure two types of films were deposited using precursor solutions with acetic acid or nitric acid as chelating agent, which are denoted as ZA and ZN, respectively.

The phase composition of the samples was studied by X-ray diffraction (XRD) with CuKα-radiation (Philips PW 1050 apparatus). The size of crystallites was calculated using Sherrer's formulae. A scanning electron microscope (SEM) JEOL JEM-200CX was used for morphology observation of the films. The photographs were taken in secondary electrons imaging mode (SEI) at 80 keV accelerating voltage. X-ray photoelectron spectroscopy (XPS) was applied to investigate the chemical composition and electronic structure of the films surface. The measurements were carried out on AXIS Supra photoelectron spectrometer (Kratos Analitycal Ltd.) using achromatic AlKα radiation with a photon energy of 1486.6 eV and charge neutralisation system. The binding energies (BE) were determined with an accuracy of ±0.1 eV, using the C1s line at 284.6 eV (adsorbed hydrocarbons). The chemical composition in the depth of the films was determined monitoring the areas and binding energies of C1s, O1s and Zr3d photoelectron peaks. Using the commercial data-processing software of Kratos Analytical Ltd. the concentrations of the different chemical elements (in atomic %) were calculated by normalizing the areas of the photoelectron peaks to their relative sensitivity factors. Transmittance and reflectance spectra of the samples were measured using UV-VIS-NIR spectrophotometer Cary 5E (Varian) in the spectral ranges 200–900 nm and 320–800 nm, respectively. The rms surface roughness values were obtained from 3D optical images taken with optical profiler Zeta-20 (Zeta Instruments). Photoluminescence measurements were performed at room temperature at excitation wavelengths from 250 nm to 280 nm with step of 10 nm with Spectrofluorometer FluoroLog3-22 (Horiba JobinYvon).

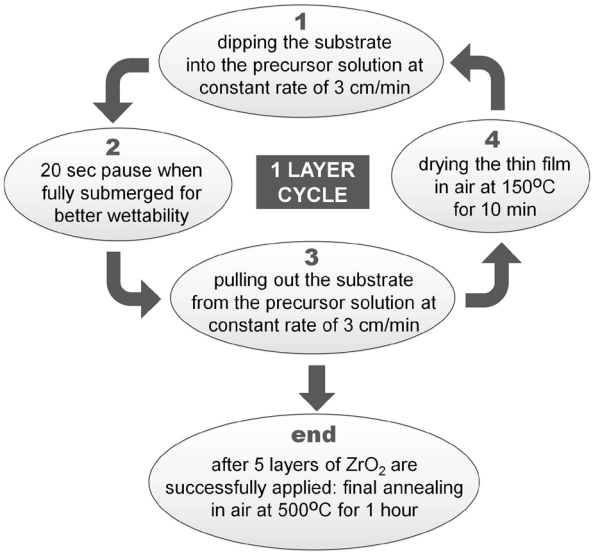

Fig. 1. Experimental procedure for preparation of 5-layered ZrO_2 thin films.

RESULTS AND DISCUSSION

Phase structure and composition

The XRD analyses revealed that all films possess tetragonal ZrO_2 crystallographic phase (JCPDS card 881007) and the corresponding XRD patterns are shown in Fig. 2. The size of the crystallites of those films obtained from solution stabilized with weak acid (CH_3COOH) are 15 nm, while in the case of strong acid stabilizer (HNO_3) the crystallites are twice as big, 32 nm. This might be the result of the double role of the acetic acid as chelating agent and catalyst of the reaction of hydrolysis condensation process. The complexing agent (CH_3COOH) retards the processes of aggregation and growth rate which leads to smaller crystallites size.

The surface composition and chemical state of the samples were investigated by XPS. Peaks of O1s, C1s and Zr3d are observed on the films surface. The O1s core level spectrum show wide peaks which are assigned to lattice oxygen in ZrO_2 (529.5 eV), adsorbed hydroxyl species (531.6 eV) and physisorbed water (534.0 eV) (Fig. 3a). The

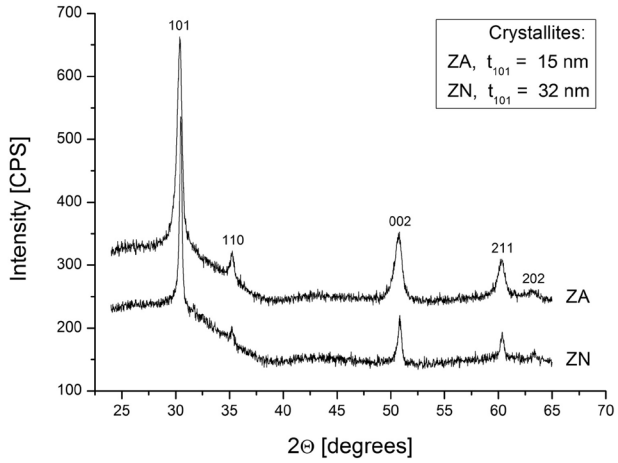

Fig. 2. XRD spectra of ZrO_2 thin films, obtained with different stabilizers.

Zr3d photoelectron spectrum shows peaks with binding energy 181.7 eV for $Zr3d_{5/2}$ and 184.1 eV for $Zr3d_{3/2}$ (Fig. 3b). The observed peaks positions, the doublet separation between the $3d_{5/2}$ and $3d_{3/2}$ peaks of ~2.4 eV are characteristic for ZrO_2. Similar results have been reported in the literature for Zr^{4+} in ZrO_2 [23]. The different chelating agents do not change the shape of the zirconia peaks. The ZrO_2 films are not stoichiometric, which is evident from the $O_{lattice}$/Zr atomic ratio (Table 1).

Table 1. Chemical composition of ZrO_2 sol-gel films

Samples	O [at.%]	Zr [at.%]	$O_{lattice}$/Zr
ZA	78.8	21.2	1.62
ZN	74.9	25.1	1.60

Surface morphology

Images revealing the surface morphology of samples ZA and ZN are presented in Fig. 4. The SEM photographs show dense ganglia-like film structure with uniform morphology. The sample obtained from the solution with weak acid exhibits formation of secondary crystallites on the surface of the film. The surface roughness was further investigated using optical profiler. The 3D optical images of the studied samples deposited on silicon substrates are presented in Fig. 5. The films are crack free with smooth morphology. Some randomly dispersed single particles with sub-micron and micron sizes could be seen on the surface mostly pronounced in films obtained with HNO_3 as a stabilizer. The rms roughness values of the films are 8.2 nm and 9.5 nm for ZA and ZN films, respectively.

Optical properties

Fig. 6 presents the transmittance spectra of the films deposited on glass substrates. As could be expected, the films are transparent in the studied spectral range with transmittance values of about 80% thus confirming the good optical quality of both films. The low amplitude of the interference peak for the ZN sample can be related to higher losses of the film that could be due to absorption or scattering. Additional measurements of optical constants are performed in order to clarify this.

Refractive index (n) and extinction coefficient (k) of the films are presented in Fig. 7. The optical constants (n and k) along with the thickness of the films (d) are determined using previously developed calculating procedure described in details in another article [24]. Briefly, non-linear curve fitting method is used for the minimization of goal func-

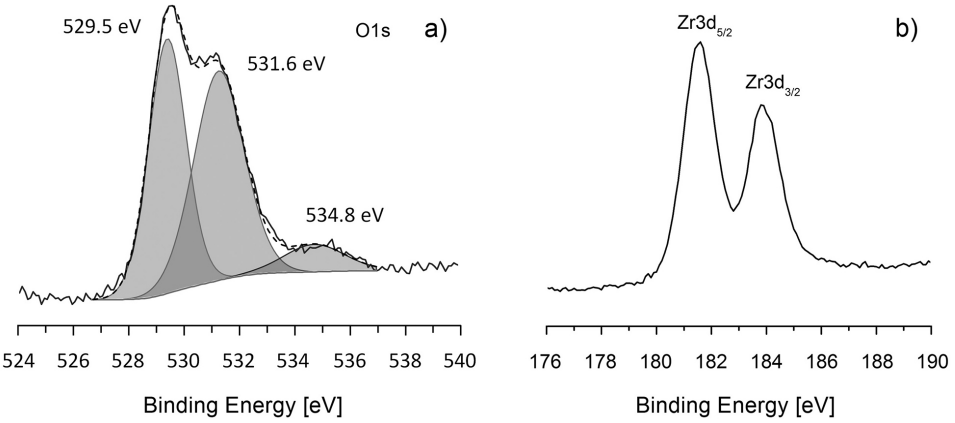

Fig. 3. Deconvolution of O1s photoelectron spectrum (*a*) and high-resolution spectrum of Zr3d of the ZrO_2 thin films (*b*).

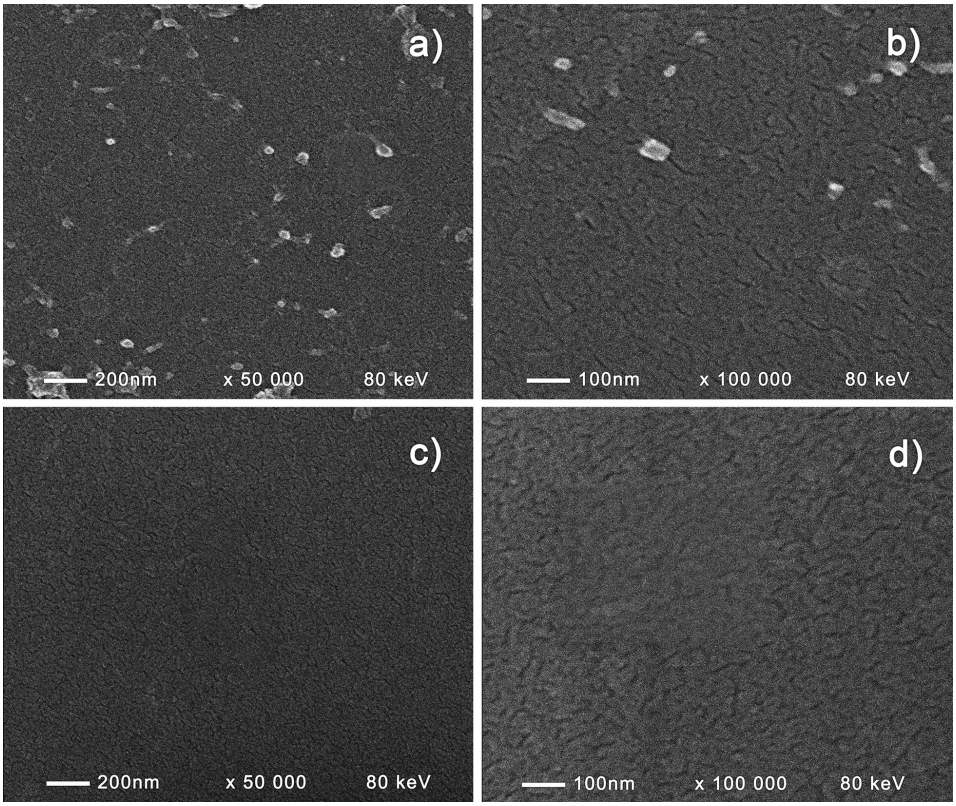

Fig. 4. SEM images of ZrO_2 thin films, obtained with acetic acid (*a*, *b*) and nitric acid (*c*, *d*).

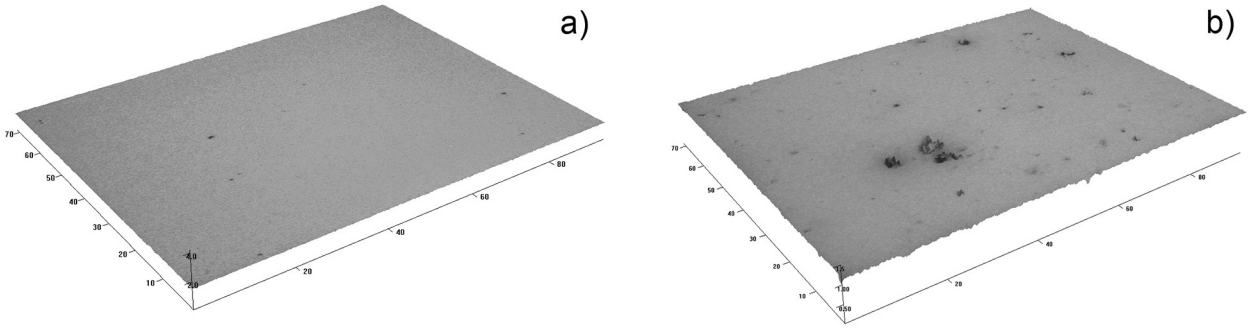

Fig. 5. 3D images of the surface of ZA (*a*) and ZN (*b*) thin films at 100 times magnification.

tion consisting of discrepancies between the measured and calculated reflectance spectra. Purposely the thin films are deposited on silicon substrates and their reflectance spectra (R) are measured at normal light incidence. The experimental errors for R, n, k and d are 0.3%, 0.005, 0.003 and 2 nm, respectively.

It is seen from Fig. 7 that for both films the dispersion curves of n and k obey normal dispersion, i.e n and k decrease with increasing of wavelength. This could be expected considering the transparency of the films in the studied spectral range. The refractive index of the films prepared using CH_3COOH is higher as compared to this prepared with HNO_3 and has values at wavelength of 600 nm of 1.672 and 1.602, respectively; the calculated thickness values are 203 nm and 165 nm, respectively. Because the thicknesses of the two films are similar, the thickness dependence of refractive index as a possible reason for the difference in n-values for the two films could be ruled out. In the visible spectral range both films have low losses with extinction coefficients at wavelength of 600 nm of 0.009 and 0.020 for ZA and ZN films, respectively. Thus, the higher losses of films prepared using HNO_3, men-

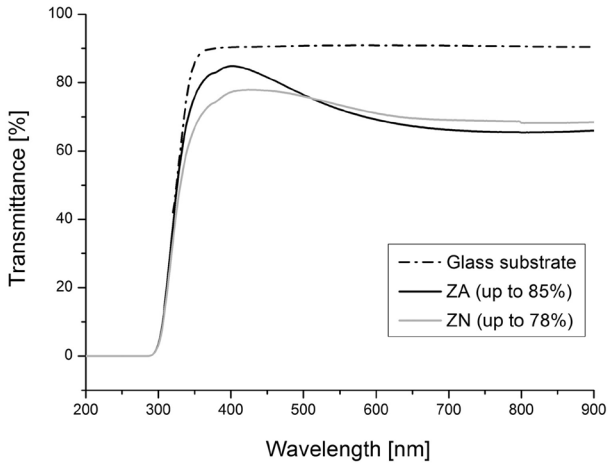

Fig. 6. Transmittance spectra of ZrO_2 thin films, obtained with different stabilizers.

tioned above, are related to higher absorption of the films. Additionally, stronger scattering losses due to the higher surface roughness of these films could also attribute to lower transmittance.

The photoluminescence spectra of the films were obtained in the wavelength range of 300–550 nm under 4 excitation energies as presented in Fig. 8. It can be seen that both samples possess broad emission band with maximum at 401 and 415 nm for ZA and ZN, respectively. The peaks are in the visible range and correspond to violet emission. Their intensity is stronger for the ZN films, due to the larger size of crystallites, as opposed to the ZA sample. Another research group has reported that the intensity of the luminescence band of ZrO_2 powders increases drastically upon increasing the crystal size [25].

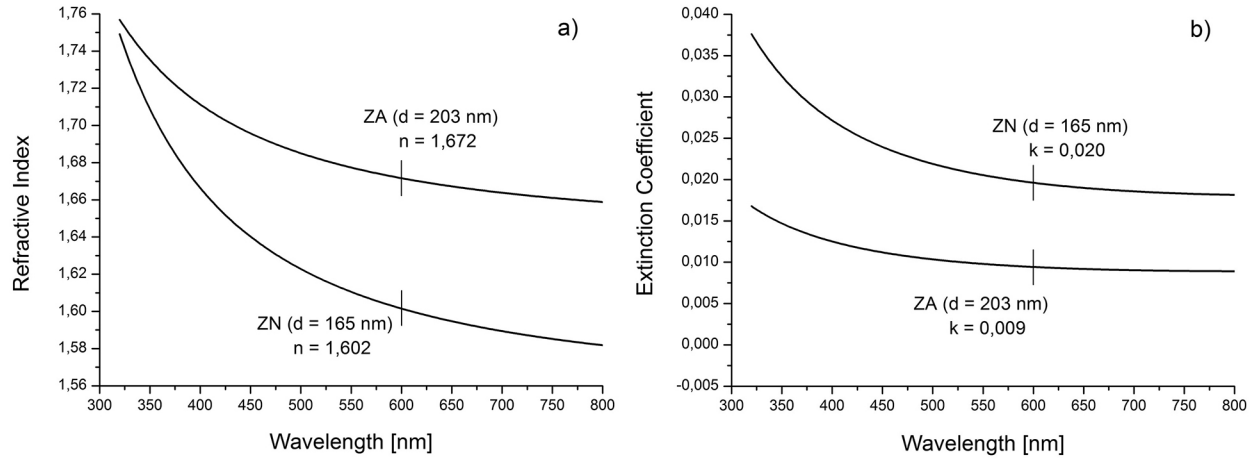

Fig. 7. Refractive index (*a*) and extinction coefficient (*b*) of ZrO_2 thin films, obtained with different stabilizers.

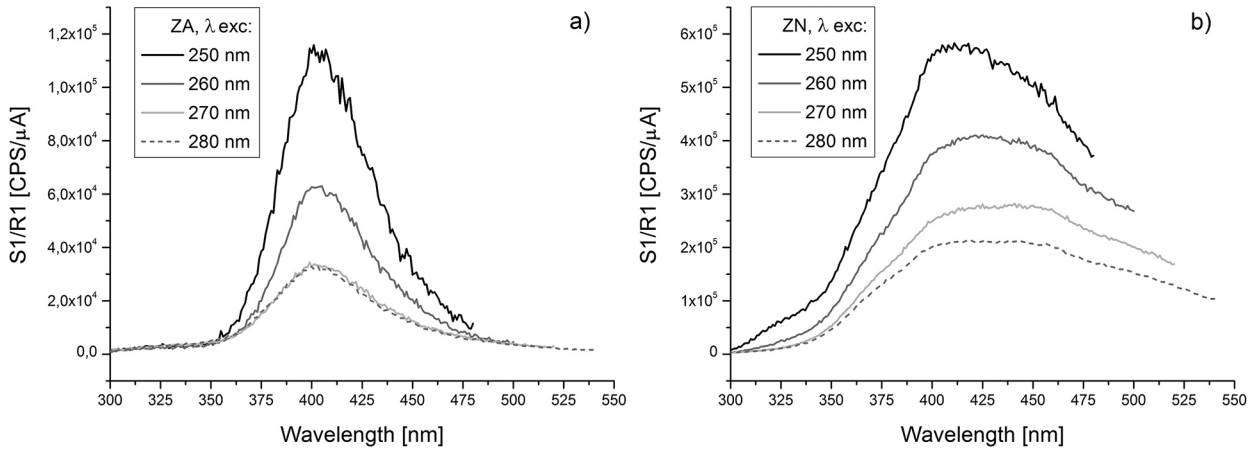

Fig. 8. Photoluminescence spectra of ZrO_2 thin films, obtained with acetic acid (*a*) and nitric acid (*b*).

The Zr^{4+} ion itself do not exhibit photoluminescence properties. The broad emission band could be attributed to the ionized oxygen vacancies in the ZrO_2 nanomaterials [26]. The XPS analysis has revealed that the ratio $O_{lattice}/Zr$ for both samples is about 1.6, suggesting the presence of oxygen defects.

It is well known that the sol-gel deposition parameters (solution composition, annealing temperature and duration, the type of catalyst, etc.) influence greatly the type of defects that occur on the films surface. That is why the emission spectra of studied samples differ from those presented in the literature [21]. Thus obtained ZrO_2 thin films could find application in photonic devices due to their luminescence properties in the short wavelength.

CONCLUSIONS

Thin nanosized homogeneous ZrO_2 films were deposited by dip coating sol-gel technique using weak or strong acid as stabilizing agents. In both cases the films crystallize in tetragonal ZrO_2 phase. The addition of strong acid (HNO_3) promotes two times larger crystallites than those obtained with weak acid (CH_3COOH). The films have dense, continuous surface with low roughness value. Both films have good optical quality with transmittance values of about 80%. The refractive indexes of the films prepared using CH_3COOH and HNO_3 are 1.672 and 1.602 respectively. The XPS analysis revealed non stoichiometric chemical composition with oxygen defects that play an important role for the photoluminescence properties. The PL spectra exhibit broad emission band with maximum at 401 and 415 nm for the samples obtained from solution with weak and strong acid, respectively. The intensity of the PL peak is stronger for the ZN films, as opposed to the ZA samples, due to the larger crystallites sizes. The observed short wavelength PL emission makes studied ZrO_2 films suitable candidates for application in light emitting devices.

REFERENCES

1. L. Liang, Y. Xu, D. Wu, Y. Sun, *Mater. Chem. Phys*., **114**, 252 (2009).
2. K. Izumi, N. Minami, Y. Uchida, *Key Eng. Mater*., **150**, 77 (1998).
3. Z. Zhang, G. Ji, Z. Shi, *Surf. Coat. Technol*., **350**, 128 (2018).
4. A. Dankeaw, G. Poungchan, M. Panapoy, B. Ksapabutr, *Sens. Actuators, B*, **242**, 202 (2017).
5. G. S. Kaliaraj, V. Vishwakarma, K. Kirubaharan, T. Dharini, B. Muthaiah, *Surf. Coat. Technol.*, **334**, 336 (2018).
6. M. Friis, C. Persson, J. Wigren, *Surf. Coat. Technol.*, **141**, 115 (2001).
7. S. Zhao, F. Ma, K. W. Xu, H. F. Liang, *J. Alloys Comp*., **453**, 453 (2008).
8. B. Hobein, F. Tietz, D. Stover, E. W. Kreutz, *J. Power Sources*, 105, 239 (2002).
9. D. J. Burleson, J. T. Roberts, W. L. Gladfelter, S. A. Campbell, R. C. Smith, *Chem. Mater*., **14**, 1269 (2002).
10. P. Stefanov, D. Stoychev, I. Valov, A. Kakanakova-Georgieva, T. S. Marinova, *Mater. Chem. Phys*., **65**, 222 (2000).
11. M. García-Hipólito, O. Alvarez-Fregoso, E. Martínez, C. Falcony, M. A. Aguilar-Frutis, *Opt. Mater*., **20**, 113 (2002).
12. J.-S. Lee, T. Matsubara, T. Sei, T. Tsuchiya, *J. Mater. Sci*., **32**, 5249 (1997).
13. C. J. Brinker, G. W. Scherer, Sol–gel science. The physics and chemistry of sol–gel processing, Academic Press, San Diego, 1990.
14. X. Wang, G. Wu, B. Zhou, J. Shen, *J. Alloys Comp*., **556**, 182 (2013).
15. G. Ehrhart, B. Capoen, O. Robbe, Ph. Boy, S. Turrell, M. Bouazaoui, *Thin Solid Films*, **496**, 227 (2006).
16. F. Davara, A. Hassankhani, M. R. Loghman-Estarki, *Ceram Int*., **39**, 2933 (2013).
17. C. Lin, C. Zhang, J. Lin, *J. Phys. Chem. C*, **111**, 3300 (2007).
18. X. Changrong, C. Huaqiang, W. Hong, Y. Pinghua, M. Guangyao, P. Dingkun, *J. Membr. Sci*., **162**, 181 (1999).
19. B. Babiarczuk, A. Szczurek, A. Donesz-Sikorska, I. Rutkowska, J. Krzak, *Surf. Coat. Technol.*, **285**, 134 (2016).
20. M. Kumar, G. B. Reddy, *AIP Adv*., **1**, 022111 (2011).
21. J. S. Lakshmi, I. J. Berlin, G. P. Daniel, P. V. Thomas, K. Joy, *Physica B*, **406**, 3050 (2011).
22. A. V. Vinogradov, V. V. Vinogradov, *J. Am. Ceram. Soc*., **97**, 290 (2014).
23. G. I. Cubillos, J. J. Olaya, M. Bethencourt, G. Cifredo, G. Blanco, *Revista Mexicana de Fısica*, **60**, 233 (2014).
24. K. Lazarova, M. Vasileva, G. Marinov, T. Babeva, *Opt. Laser Technol*., **58**, 114 (2014).
25. A. Patra, C. S. Friend, R. Kapoor, P. N. Prasad, *Appl. Phys. Lett*., **83**, 284 (2003).
26. L. Kumari, W. Z. Li, J. M. Xu, R. M. Leblanc, D. Z. Wang, Y. Li, H. Guo, J. Zhang, *Cryst. Growth Des*., **9**, 3874 (2009).